



Cite this: *Anal. Methods*, 2015, **7**, 7363

## Microelemental characterisation of Aboriginal Australian natural Fe oxide pigments

R. S. Popelka-Filcoff,<sup>\*a</sup> C. E. Lenehan,<sup>a</sup> E. Lombi,<sup>b</sup> E. Donner,<sup>b</sup> D. L. Howard,<sup>c</sup> M. D. de Jonge,<sup>c</sup> D. Paterson,<sup>c</sup> K. Walshe<sup>d</sup> and A. Pring<sup>ad</sup>

This manuscript presents the first comprehensive microcharacterisation of Fe oxide minerals used in Aboriginal Australian mineral pigments. The combination of X-ray fluorescence microscopy (XFM) and light microscopy provides a broad characterisation as well as the ability to spatially match visual observation with elemental composition. A novel method for casting pigment samples in a pattern on a slide was used for consistent elemental mapping. Semiquantitative bulk data was also collected and compared to the microscopic and microelemental data. These analyses demonstrate the ability to document the variability in ochre pigments in Australia, as well as which elements drive the variation within and between ochre source locations. The methods developed provide a more comprehensive understanding of other complex natural mineral pigments worldwide.

Received 16th June 2015  
Accepted 30th July 2015

DOI: 10.1039/c5ay01547b

[www.rsc.org/methods](http://www.rsc.org/methods)

## Introduction

Ochre and related natural Fe oxide pigments are a significant material in Indigenous cultures worldwide. Ochre pigments are utilised for their durability and widespread availability as observed in rock art from thousands of years ago, as well as their cultural symbolism in colour in modern times. In Aboriginal Australia, Fe-based mineral pigments are found in nearly every cultural context from a diverse array of cultural objects (shields, spears, boomerangs, bark paintings and others), in archaeological remains and rock art. Ochre continues to have strong cultural traditions in the present day. Examples of this include the use of natural mineral pigments in contemporary art centres such as those in the Kimberley region of Western Australia, and the use of ochre pigments on the body.<sup>1,2</sup>

To visual inspection (approximately 10 cm distance) natural ochre pigments can appear to be homogeneous with a solid coverage of the substrate at a uniform thickness and particle size and shape. However under magnification, it can be observed that the pigments are composed of a range of particle shapes and sizes, and in many cases a range of colours. This distribution of natural pigmented particles, often caused by accessory minerals has not been well characterised.

In addition, the pigments adhere to the substrate with a degree of variation depending on the method of application,

type of substrate, type of binder and any variability in the substrate itself. Variation in these factors include whether the pigment is applied by hand or by brush or other implement. Typical substrates for Aboriginal Australian objects include bark, wood and plant fibres, or in the case of rock art, natural rock substrates. Various types of binders were also used for mixing pigments, which include water and various plant and animal materials.<sup>3,4</sup>

Ochre is a complex mixture of Fe oxides and other minerals that can include calcite, gypsum, clays and feldspars. Iron oxides occur in varied geological formations, including red beds, banded iron formations, gossans and sediments. Ochre formations are also prevalent in soils that can contain several Fe-oxide minerals simultaneously.<sup>5</sup> Each ochre carries a chemical and mineralogical "signature" that reflect the digenetic processes of the source. Sampling across a deposit provides information on the local variability of the geochemical signature. It has been demonstrated that a single sample from a site is not necessarily characteristic of a single geochemical composition of the site, due to geological variability within the mine or quarry.<sup>6,7</sup> Characterisation of multiple samples from within a site is essential to give a more complete assessment of the diversity within the site. For these samples, neutron activation analysis (NAA) provides elemental data on variability between bulk samples on the order of 50–100 mg as single concentration values for 30+ elements per sample. Previous studies have demonstrated that NAA data used with multivariate statistical techniques can characterise individual sources geochemistry on the bulk scale as well as differentiate ochre sites from each other. While these data are valuable for understanding the source geochemical variability on a large scale, the variability at the micron scale of the ochre cannot be

<sup>a</sup>School of Chemical and Physical Sciences, Flinders University, Adelaide, SA, Australia. E-mail: rachel.popelka@flinders.edu.au

<sup>b</sup>Centre for Environmental Risk Assessment and Remediation, University of South Australia, Adelaide, SA, Australia

<sup>c</sup>Australian Synchrotron, Clayton, VIC, Australia

<sup>d</sup>South Australian Museum, Adelaide, SA, Australia



determined by NAA. The Fe oxides in ochre are known to be admixed with a range of accessory minerals such as clays, calcites and others, however the contribution of each mineral to the characteristic geochemical signatures is unknown.<sup>8</sup> Therefore an elemental examination of the ochre on the micron level is essential to understand not only the elemental composition of the ochre material and minerals, but also the inherent variability of micron-sized particles of minerals that compose the complex ochre mixture. An analysis of this scale provides not only information on the elemental distribution of the sample, but also spatial and morphological information on the elemental distributions. While recent advances in scanning electron microscopy (SEM) coupled with elemental analysis (EDAX), have allowed elemental raster mapping of samples, the resolution is generally on the order of 100 microns. In addition, the maps produced are low resolution and not representative of the fine structure of the surface. Samples introduced to the SEM are limited to those that are small enough (<2 mm diameter stub) to fit into the chamber and that can tolerate high vacuum conditions, and potentially coated with carbon or gold for imaging purposes. None of the above conditions are acceptable for artefacts or ochre from cultural heritage materials.

X-ray fluorescence microscopy (XFM) as a form of micro-XRF analysis performed at the Australian Synchrotron (AS) provides the necessary analysis on the elemental level to understand the original source variability of complex natural mineral ochre pigments. Using the Maia detector provides high resolution mapping of individual particles inherent in the original sourced or archaeological ochre sample. In addition, unlike NAA, XFM requires only micrograms of material and is non destructive. XFM can analyse larger areas (on the order of cm) on many sample types with much higher sensitivity than SEM-EDAX. These capabilities are ideal for cases where trace elements can be diagnostic in terms of fingerprinting and where these trace elemental distributions may be smaller than SEM resolution of 100 micron or where the presence of the element was unknown. XFM can further be used to analyse cultural heritage artefacts as well as individual pigment samples, which is not possible using SEM-EDAX or NAA. A comparison of the individual pigment samples to the artefact provides a valuable advantage of a direct data comparison and technique from sample to artifact. A few prior studies have demonstrated successful application of XFM to cultural pigments.<sup>9-13</sup>

Recently there have been several studies that have explored a range of techniques with the aim of developing methods for establishing the provenance of ochre and pigments with archaeological and ethnographic associations including possible trade routes.<sup>1,6,7,14-16</sup> However, many of these studies are based on the analysis of the bulk of the material, with such techniques as neutron activation analysis (NAA) and laser ablation inductively coupled plasma mass spectrometry (LA-ICP-MS).<sup>6,7,17</sup> However there is one recent study on the characterisation of Australian ochre using synchrotron XRD and PIXE.<sup>18</sup> There are a few studies utilising microscopy of Fe oxides, however these concern the mineral properties and not the cultural aspects.<sup>5</sup>

This manuscript will focus on the multiple samples taken from five well known and documented ochre sources from Australia: Bookartoo (also spelled Bukartu and Pukatoo) (South Australia), Karrku (Northern Territory), Moana (South Australia), Pine Point (South Australia) and Wilgie Mia (Western Australia). Samples from these sites have been collected over several years by researchers including M. Nobbs, P. Jones, M. Smith and others associated with the South Australian Museum and the Western Australian Museum.<sup>6,19-26</sup>

Here we describe the first systematic microanalysis and documentation of ochre samples towards a more complete understanding and micro-characterisation of Aboriginal Australian ochre pigments. These data provide a foundation data set for feasibility studies for the in-beam analysis of Aboriginal Australian objects from several of the most significant ochre quarries in Australia and enhances knowledge of this inherently complex material. This study also expands the capability of the method towards understanding complex geological systems and formations, which may also inform environmental influence on Fe-oxide deposits.

## Experimental

### Sample selection

A suite of ochre samples has been assembled from individual researchers as well as from the South Australian Museum Archaeology and Ethnographic collections.<sup>6,19-26</sup> The majority of these samples have also been analysed by complementary techniques such as NAA.<sup>6,24</sup> From this larger combined collection, 165 samples were chosen for analysis by X-ray fluorescence microscopy (XFM). These 165 samples represented source (site) samples as well as samples from archaeological context. Sources in this project are defined as the original "quarry" or geological formation of the ochre material; therefore these samples were collected directly from the source in the field or presumed to be. On the other hand, archaeological samples may or may not be from the original quarry as they may have been exchanged through cultural networks.

Located in the Flinders Ranges, South Australia, Bookartoo samples have been collected from this extensive site over different time periods and therefore likely different locations within the site.<sup>16,23,27</sup> OCH050 and OCH24 were collected by Margaret Nobbs, whereas the OCH075-76-79A and OCH255 series are from Mike Smith. Karrku, located in the Northern Territory, is the local name for "ochre".<sup>28</sup> The samples were collected by Mike Smith and Barry Fankhauser as part of ochre characterisation studies completed in the 1990s. These samples were collected over a period of two years from the site. Moana is an exposed coastal site near Adelaide (South Australia) and therefore is subject to more intense weathering and effects of the ocean. Geologically, it is a sedimentary site as opposed to Karrku and Bookartoo, which are weathered banded iron formations. Similarly to Moana, Pine Point is an exposed and therefore weathered site on the coast of Yorke Peninsula (South Australia). Wilgie Mia (Western Australia), also a weathered banded iron formation is perhaps the best-known site due to the quality of the ochre and the large scale of the site.<sup>29</sup>



## Sample preparation

In order to minimise the variation in the original state of the material, a consistent method was implemented to standardise the preparation of the ochre minerals for microscopy and XFM analysis.

All samples were hand ground in a Brazilian agate mortar and pestle to a consistent particle size powder. Samples were dried overnight in a 100 °C oven and stored in glass vials. All samples were sieved to <250 micron using individually cut disposable plastic mesh screens to minimise cross contamination between samples. This step was performed to remove potentially large particles as well as organic material such as grasses and plant fibres. Additionally, the particle size of 250 micron was chosen as a likely maximum size for the use of Indigenous pigments on objects. However, depending on the origins of the pigment and the particular characteristics of the mineral, a variation in particle size and distribution is expected.

A standard microscopy quartz slide (2 × 1 inches, 5.08 × 2.54 cm) was prepared by sanding it with fine grit sandpaper to aid in the attachment of the epoxy cast mineral to the slide. A grid was laid out on the slide with space for 45 samples per slide, in 15 columns and 3 rows (Fig. 1). The samples were cast individually in epoxy on a quartz slide in even distribution for ease of analysis by XFM. Duplicates of each slide were also made.

A grid mask was designed to affix to the slide to aid the casting of the samples, to maintain the pattern of 2 × 2 mm squares for each individual sample, separated by 0.5 mm. The grid mask was designed by CAD design and produced in a polymer mask “sticker”. The individual blocks were cut by a blade and removed individually, and each individual sticker was applied to the front face of each slide.

In order to affix the samples permanently to the slides, approximately 5–10 milligrams of each sample were mixed individually with Petropoxy 154 epoxy (Burnham Petrographics) in a glass vial with a glass stirrer in a 50/50 volume. This epoxy was chosen for its known capabilities in mineral slide preparation, fast set time as well as its relatively contaminant-free substrate that would not introduce further elemental impurities. After allowing the epoxy to cure for approximately 60 minutes in an 80 °C oven, the samples were applied manually, with the aid of a binocular microscope to each individual well, filling each well with a layer of sample. After the first applications had solidified a second layer for individual samples was applied to each well. After a complete curing of the epoxy to hardness in an 80 °C oven for 30 min, the entire slide was



Fig. 2 An example of completed slide with the 45 individual ochre samples cast in Petropoxy resin. Each square is approximately 2 mm square, with 0.5 mm between the squares.

allowed to cool and the epoxy to set for several hours until completely cured. The “sticker” mask was then removed with a blade. The entire slide was then cured on a 130 °C hotplate for a few minutes. The slides were then polished to approximately 80–100 micron thickness to achieve a consistent thickness of epoxy samples. Fig. 2 is an example of one completed slide set with 45 ochre samples. It is expected that the samples will be heterogeneous across the individual sampling squares, but this sampling method will be more representative of a cultural application of a natural ochre pigment to an object. Although there is slight variation in the shape and coverage of each sample, the area in the centre of the square is representative of each sample.

## XFM beam line parameters

The experiment utilised the standard set up of the XFM experimental parameters with the Maia detector (a 384-element array of 1 × 1 mm Si detectors, oriented axially in backscatter geometry, which is 180° to beam).<sup>11,30</sup> X-ray focusing was achieved with Kirkpatrick-Baez mirrors, which provide longer working distance and high sensitivity requirements as compared to other X-ray analysis setups.<sup>30</sup> The Australian Synchrotron operated at 3 GeV with a stored current of 150–200 mA. During these experiments, the XFM beam had an incident energy of 18.5 keV and a flux of approximately  $8 \times 10^8$  photons per second.

For the experimental set-up, the individual polished slides were attached to the plexiglass sample holder frame used for XFM measurements. This setup is regularly used for the experiments and also allows for a set distance from the slides to the beam and detector.

Since the area of each slide is relatively small, a smaller step size was chosen to maximise the characterisation of the sub-micron areas of pigment. During the experiments the beam size was 2 micron. The samples were analysed at a rate of 0.768 mm per second with a step size of 2 microns. A sampling area of

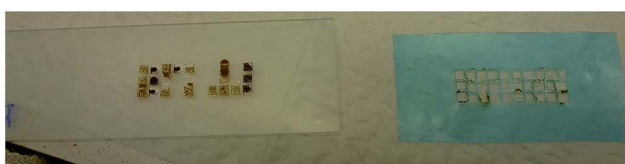


Fig. 1 A demonstration slide displaying the sticker mask (light blue, right), with ochre squares cast in resin remaining on the slide after sticker removal (left).



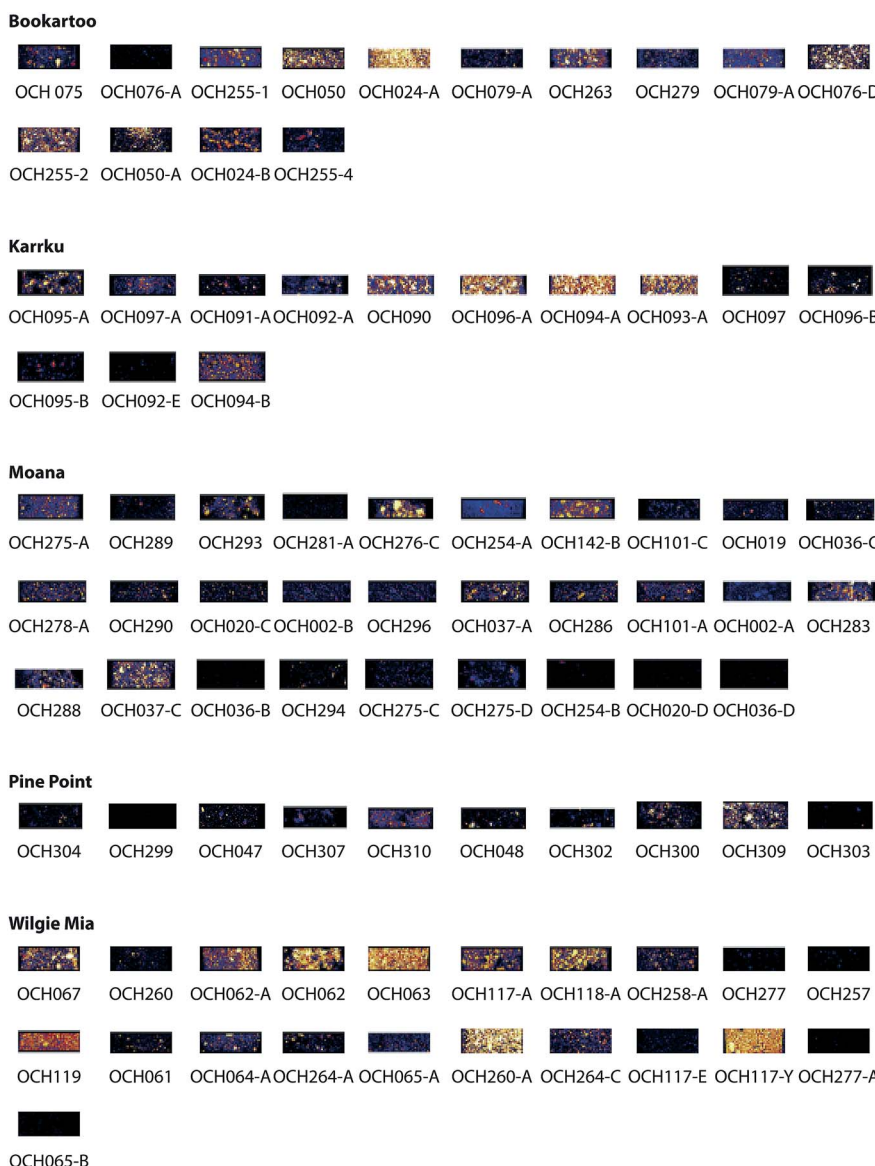


Fig. 3 Microelemental map of Fe for samples from the sites analysed in this study. Images are false coloured to demonstrate relative concentration intensities, with black the lowest and white/yellow the highest. Sites are highlighted in each image. (a) Bookartoo (b) Karrku (c) Moana (d) Pine Point (e) Wilgie Mia.

approximately 0.7 mm high strip through the centre of each row of the samples was chosen for a consistent measurement area of each row and to minimise variation. An area of  $36.9 \times 0.7$  mm was analysed for each row of the slides, producing a total of 11 rows of 15 samples (165 samples total). The slides were analyzed in three separate experiments, but with similar conditions. Data analysis was accomplished using the GeoPIXE software package.<sup>11,30</sup>

The elements measured in this study included As, Ca, Cr, Cu, Fe, Ga, Mn, Pb (L line), Rb, Sc, Se, Sr, Ti, V, and Zn. For each pixel, the full XRF spectrum is collected. GeoPIXE is used to deconvolute these individual spectra into elemental concentration maps. Relative concentrations of each element or combinations of elements are indicated by colour and intensity of the colour. For each point in the image as well as for areas in

the image, GeoPIXE can determine semiquantitative values of the elements analysed. A rectangular area of  $1.664 \text{ mm wide} \times 0.608 \text{ mm high}$  was used to calculate the semiquantitative areas and limits of detection for each element for each pigment square. Semiquantitative data were used to compare pigments to each other as well as to compositional data from other techniques.

### Light microscopy

The slides used for XFM analyses were also studied in the light microscopy analysis to provide a direct comparison between the elemental maps and microscopy images. The slides were viewed through an Olympus CX41 transmitted light microscope at  $100\times$ . Digital images were captured using an Olympus DP21 camera.



Fig. 4 Microelemental map of Ca for samples from the sites analysed in this study. Images are false coloured to demonstrate relative concentration intensities, with black the lowest and white/yellow the highest. Sites are highlighted in each image. (a) Bookartoo (b) Karrku (c) Moana (d) Pine Point (e) Wilgie Mia.

## Results and discussion

### XFM images

Images from the XFM analysis demonstrated the inherent variability of the ochre samples across sources and between sources. While 165 samples were analysed, individual examples from each highlighted site are selected for discussion (Fig. 3–6).

Data were acquired for all 15 elements, however, some elements demonstrated very low concentrations and therefore very little data in the maps. These results indicate that the elements in the ochre pigment sample are below detection limits of the technique. Of the elements examined, data for the maps were consistently found for As, Ca, Cr Fe, Mn, Ti, and V. Elemental concentrations for Cu, Ga, Pb, Sc, Se, Sr and Zn were generally close to or below detection limits for the sites

highlighted in this study; therefore images are not presented. Prior to this study data for Cu and Pb were unknown for ochre samples, as NAA is not able to analyse for these two elements. These data reveal that Cu and Pb are not diagnostic for identifying or characterising the ochre origin and these elements will not be discussed further. Table 1 presents the semiquantitative data for the elements analysed and for the sites discussed. The range of values generally agrees with other bulk methods such as NAA within 10–20%.<sup>6,7</sup> However there is not a perfect agreement with the bulk methods. NAA is a traceable method that uses certified and reference standards for calculation of values and uncertainties. GeoPIXE utilises a user-supplied model of the specimen matrix, in which the matrix composition ( $Fe_2O_3$ ), its density ( $5.24 \text{ g cm}^{-3}$ ), and uniform thickness ( $100 \mu\text{m}$ ) are used to model the X-ray fluorescence yields. Deviations of the



Fig. 5 Microelemental map of Rb for samples from the sites analysed in this study. Images are false coloured to demonstrate relative concentration intensities, with black the lowest and white/yellow the highest. Sites are highlighted in each image. (a) Bookartoo (b) Karrku (c) Moana (d) Pine Point (e) Wilgie Mia.

specimen from the assumed matrix parameters will lead to a less accurate determination of sample concentration. The matrix and its thickness will vary between samples, thus we regard the results as semiquantitative. We note that assuming hematite or goethite as a matrix makes negligible difference to the determined concentration, but a grossly different matrix such as silicate will be significant. The sampling size between the two methods is quite different, on the order of mg for XFM as compared to at least 50 mg for NAA, which will influence the samples representation to the bulk. In particular for XFM, the sample is further diluted approximately 1 : 1 by volume in the epoxy resin, therefore affecting the calculations by GeoPIXE. In general, this will reduce the concentrations by approximately one half for iron and heavier elements, reduce by 30% for V-Cr and increase Ca, Ti by about 30%.

Discussion of the elemental maps will follow by element. A further discussion of the sites and their archaeology is discussed elsewhere in the literature.

#### Fe

As Fe is the main constituent of Fe-oxide ochre pigments, the elemental maps of Fe were studied in more detail to identify trends in the data. Concentrations ranged from 26 ppm to 45%.

#### Bookartoo

Variations can be observed in the overall intensity of the false colour maps but this is likely an effect of the variability in the scaling of the image brightness relative to other samples rather than a reflection of the actual concentration of Fe in each sample (see below). The samples exhibit a dense coverage of



Fig. 6 Microelemental map of Ca, Fe and V for samples from the sites analysed in this study. Red indicates Ca, green indicates Fe and blue indicates V. Images are false coloured to demonstrate relative concentration intensities, with black the lowest and the indicated colour the highest. Sites are highlighted in each image. (a) Bookartoo (b) Karrku (c) Moana (d) Pine Point (e) Wilgie Mia.

small iron oxide particles with some larger platy iron oxide particles of higher concentration. These data support earlier suggestions of “micaceous” ochre observed from the site.<sup>19,23,27</sup> This ochre is visually a deep purple red, however yellow ochre is also found at this site. OCH079-A is an example of yellow ochre, and its lower Fe concentration indicated is composition of goethite [ $\alpha$ -FeO(OH)] rather than hematite ( $\text{Fe}_2\text{O}_3$ ), or admixture of yellow iron pigments with other lower-Fe minerals such as siderite ( $\text{FeCO}_3$ ) or jarosite-group minerals ( $\text{XFe}_3(\text{SO}_4)_2(\text{OH})_6$ ) with  $\text{X} = \text{K, Na, Pb}$  etc.

### Karrku

Samples OCH 092-A and OCH 090, OCH096 and OCH 094-A display variation in particle size and shape. A plausible reason for this is that the samples were collected during two different

campaigns in 1996 and 1998 by Mike Smith *et al.*; therefore the variation likely reflects different sampling locations. OCH090 and OCH 092 also display more voids as compared to OCH-96-A and OCH094-A, which are more densely covered in Fe concentration. The site is known to contain soft earthy specular hematite between quartzite and is mined in a cave location.<sup>26</sup>

### Moana

Samples from the sites were obtained from the South Australian Museum, Mike Smith and the Margaret Nobbs collection. OCH020, OCH036, OCH037, OCH019, and OCH278A are from the Nobbs surveys. Remarkably, they demonstrate very low, if any, Fe signal in the elemental maps except for OCH037-A and OCH037-C, which are sub samples from a larger sample. OCH101-A and OCH 101-A were collected by Mike Smith, and



**Table 1** Semiquantitative data (in ppm for each element) for each ochre sample as calculated by GeoPIXE, organised by site name. Each area was 1.664 mm wide  $\times$  0.608 mm high on each square. Se and Ge and Cu were eliminated from the data set as all values were below detection limits

ID	Site	Ca	Sc	Ti	V	Cr	Mn	Fe	Cu	Zn	As	Rb	Sr	Pb	Pb													
		Ca	LOD	Sc	LOD	V	LOD	Cr	LOD	Mn	LOD	Fe	LOD	Cu	LOD	Zn	LOD	As	LOD	Rb	LOD	Sr	LOD	Pb				
OCH075	Bookartoo	33.081	35	<LOD	9	232	4	<LOD	2	1325	3	33.350	10	<LOD	1	5.8	0.7	<LOD	0.3	18.6	0.4	<LOD	0.8	<LOD	0.8			
OCH076- Bookartoo		46.454	43	<LOD	10	1299	6	551	4	299	2	7989	8	18.0716	13	<LOD	2	<LOD	1	<LOD	0.9	<LOD	0.3	<LOD	0.4	71	1	
A	OCH078- Bookartoo	9315	86	4	22	1703	5	1373	2	374	1	22.758	4	25.1427	8	<LOD	2	60.8	1	<LOD	0.9	26.8	0.4	36.6	0.5	385	1	
A	OCH263 Bookartoo	<LOD	39	263	11	810	5	529	3	213	2	17.044	7	17.5920	14	<LOD	2	<LOD	0.9	25.2	0.4	16.9	0.5	23.3	1			
OCH279 Bookartoo	<LOD	37	<LOD	10	566	4	<LOD	2	<LOD	1	2688	4	25.931	10	<LOD	2	<LOD	1	<LOD	0.8	22.9	0.4	30.2	0.5	31.6	1		
OCH079- Bookartoo	1800	51	<LOD	14	829	5	<LOD	2	<LOD	2	5040	5	48.047	14	<LOD	2	<LOD	1	<LOD	0.8	66.3	0.4	39.7	0.6	44.5	1		
A	OCH076- Bookartoo	<LOD	8	<LOD	4	101	3	209	2	128	1	1745	3	59.089	11	<LOD	0.9	<LOD	0.7	<LOD	0.5	0.87	0.2	<LOD	0.3	59.8	0.7	
D	OCH255- Bulkartu	89.638	60	<LOD	17	1625	7	633	4	187	3	17.226	10	18.9012	14	<LOD	2	738	3	<LOD	1	11.3	0.5	240	0.7	418	2	
1	OCH255- Bulkartu	18.719	23	<LOD	7	222	3	267	2	142	1	2076	4	62.840	11	<LOD	1	436	2	35.4	0.6	<LOD	0.2	54.7	0.3	54.9	0.7	
4	OCH255- Bulkartu	23.185	26	<LOD	7	130	3	146	2	95	1	1515	3	49.260	10	<LOD	1	189	1	<LOD	0.5	<LOD	0.2	41.2	0.3	27.7	0.7	
2	OCH095- Karrku	13.693	24	<LOD	7	701	4	<LOD	2	<LOD	1	4937	5	68.427	12	<LOD	1	<LOD	0.7	132	0.5	290	0.6	22.7	0.9			
A	OCH095- Karrku	<LOD	8	<LOD	3	84.4	2	<LOD	1	51.4	0.9	937	3	33.647	9	<LOD	0.9	<LOD	0.7	<LOD	0.5	13.3	0.3	14	0.3	12.5	0.6	
B	OCH092- Karrku	<LOD	6	<LOD	3	<LOD	2	<LOD	1	<LOD	0.7	112	1	7100	4	<LOD	0.9	<LOD	0.7	<LOD	0.4	9.49	0.2	13.7	0.3	<LOD	0.6	
E	OCH094- Karrku	789	11	99	6	695	4	533	3	433	2	4730	5	161.845	11	<LOD	1	<LOD	0.7	<LOD	0.6	17.6	0.3	<LOD	0.3	212	0.9	
B	OCH097 Karrku	<LOD	6	<LOD	3	<LOD	2	<LOD	0.9	<LOD	0.6	99.3	1	6676	4	<LOD	0.9	<LOD	0.7	<LOD	0.4	3.96	0.2	16.9	0.3	<LOD	0.6	
OCH096- Karrku	355	8	<LOD	3	121	2	<LOD	1	<LOD	0.8	312	2	13.431	6	<LOD	0.9	<LOD	0.7	<LOD	0.4	35.6	0.3	73.3	0.4	5.8	0.6		
B	OCH090 Karrku #6	<LOD	16	<LOD	8	<LOD	6	<LOD	3	<LOD	2	374	8	4847	14	<LOD	2	<LOD	1	<LOD	0.9	30.3	0.5	34	0.6	75.8	1	
OCH091- Karrku 96/1	<LOD	16	<LOD	5	295	3	<LOD	2	<LOD	1	2948	3	28.343	7	<LOD	1	<LOD	0.9	<LOD	0.6	121	0.4	297	0.5	75.2	0.8		
A	OCH092- Karrku 96/2	<LOD	13	<LOD	5	841	4	<LOD	2	<LOD	1	418	4	5849	9	<LOD	2	<LOD	1	<LOD	0.8	25.4	0.5	65.7	0.5	41.2	1	
A	OCH093- Karrku 98/2	<LOD	15	398	8	1336	6	<LOD	3	<LOD	2	3671	8	35.411	14	<LOD	2	<LOD	1	24.1	0.8	26.2	0.4	30	0.5	21.8	1	
A	OCH094- Karrku 98/3	159	16	49	8	904	6	363	4	253	3	15.463	9	146.188	14	<LOD	2	<LOD	1	<LOD	0.9	61.4	0.4	20.9	0.5	74.2	1	
A	OCH096- Karrku 98/5	<LOD	16	189	8	1252	6	45	4	28.9	3	7168	9	70.166	14	<LOD	2	<LOD	1	<LOD	0.9	75.1	0.4	45.2	0.5	64.5	1	
A	OCH097- Karrku JW	<LOD	14	<LOD	8	1098	5	<LOD	3	<LOD	2	4603	5	41.880	12	<LOD	2	<LOD	1	<LOD	0.8	212	0.6	368	0.8	81.6	1	
A	OCH062- Little Wilgie	32.545	35	<LOD	8	820	5	80	3	247	2	6945	7	157.272	13	<LOD	2	<LOD	1	<LOD	0.8	<LOD	0.3	<LOD	0.3	58.6	1	
A	Mia	OCH062 Little Wilgie	41.302	39	<LOD	9	1125	6	157	3	337	2	8134	7	191.268	13	<LOD	2	<LOD	2	<LOD	0.9	<LOD	0.3	<LOD	0.3	96.8	1
Mia	OCH062 Little Wilgie	41.302	39	<LOD	9	1125	6	157	3	337	2	8134	7	191.268	13	<LOD	2	<LOD	2	<LOD	0.9	<LOD	0.3	<LOD	0.3	96.8	1	



Table 1 (Contd.)

ID	Site	Ca	Sc	Ti	V	Cr	Mn	Fe	Cu	Zn	As	Rb	Sr	Pb	
		Ca LOD	Sc LOD	Ti LOD	V LOD	Cr LOD	Mn LOD	Fe LOD	Cu LOD	Zn LOD	As LOD	Rb LOD	Sr LOD	Pb LOD	
OCH275- Moana	A	8852 21	<LOD 6	664 4	<LOD 2	<LOD 1	1298 3	33 322 10	<LOD 1	<LOD 1	<LOD 0.6	15.5	0.3	<LOD 0.3	
OCH289 Moana	A	3324 15	<LOD 5	<LOD 3	<LOD 1	1839 3	25 285 8	<LOD 2	<LOD 1	<LOD 0.5	<LOD 0.3	<LOD 0.3	<LOD 0.3	<LOD 0.7	
OCH293 Moana	A	10 554 22	<LOD 6	575 4	<LOD 2	<LOD 1	4071 5	55 829 12	<LOD 1	<LOD 1	<LOD 0.6	10	0.3	<LOD 0.3	<LOD 0.8
OCH281- Moana	A	2134 14	<LOD 5	379 3	<LOD 1	<LOD 0.9	220 2	8618 5	<LOD 1	<LOD 1	<LOD 0.6	47	0.4	6.7	<LOD 0.8
OCH278- Moana	A	<LOD 20	<LOD 6	910 4	<LOD 2	9.8 1	6152 4	60 005 10	<LOD 1	<LOD 1	<LOD 0.6	75.1	0.4	33.1	0.3
OCH290 Moana	A	<LOD 15	<LOD 5	632 3	<LOD 1	<LOD 1	3701 3	36 440 8	19.3 2	35.8 1	<LOD 0.6	27.5	0.3	32.9	0.3
OCH002- Moana	B	<LOD 13	<LOD 5	554 3	<LOD 1	<LOD 0.9	1444 2	14 622 5	<LOD 1	<LOD 1	<LOD 0.6	97.3	0.4	42.8	0.3
OCH296 Moana	B	<LOD 9	<LOD 3	<LOD 2	<LOD 1	<LOD 0.7	374 1	4847 2	<LOD 1	<LOD 1	<LOD 0.6	30.3	0.3	34	0.3
OCH037- Moana	A	<LOD 20	189 6	1252 4	45 2	28.9 1	7168 4	70 166 10	<LOD 1	<LOD 1	<LOD 0.6	75.1	0.3	45.2	0.3
OCH286 Moana	A	<LOD 23	<LOD 6	453 4	214 2	88 1	9979 5	99 019 12	<LOD 1	<LOD 1	19.7 0.7	25.4	0.3	27	0.3
OCH101- Moana	A	1800 17	<LOD 5	829 3	<LOD 2	<LOD 1	5040 3	48 047 8	<LOD 1	<LOD 1	<LOD 0.6	66.3	0.3	39.7	0.3
OCH002- Moana	A	<LOD 14	<LOD 6	632 5	<LOD 2	<LOD 1	3701 3	36 440 8	19.3 2	35.8 1	<LOD 0.8	27.5	0.5	32.9	0.5
OCH283 Moana	A	<LOD 13	<LOD 7	50 5	72.3 2	19.4 2	6935 5	67 894 14	<LOD 2	<LOD 1	<LOD 0.8	19.9	0.4	21.9	0.5
OCH288 Moana	B	<LOD 12	<LOD 6	554 4	<LOD 2	<LOD 1	1444 5	14 622 12	<LOD 2	<LOD 1	<LOD 0.8	97.3	0.4	42.8	0.5
OCH276- Moana	C	1229 19	848 10	1964 8	1031 4	524 3	26 945 13	329 089 14	<LOD 2	539 2	<LOD 1	71.2	0.5	16.2	0.5
OCH254- Moana	A	3214 19	<LOD 8	860 6	459 3	174 2	15 159 10	165 377 14	<LOD 2	<LOD 1	413 1	37.3	0.4	890	1
OCH142- Moana	B	1031 17	494 9	2169 7	293 3	148 2	11 048 8	120 230 14	<LOD 2	<LOD 1	<LOD 1	134	0.6	70.5	0.5
OCH019 Moana	C	<LOD 11	<LOD 6	129 4	<LOD 2	<LOD 1	2400 4	22 190 9	<LOD 2	<LOD 1	<LOD 0.8	50	0.5	32.2	0.5
OCH036- Moana	A	<LOD 10	4 7	665 5	<LOD 2	<LOD 1	491 3	5879 5	<LOD 2	<LOD 1	<LOD 0.8	28.7	0.4	51.6	0.5
OCH275- Moana	C	2238 9	<LOD 4	54.2 2	0.8 1	53.9 0.9	982 3	35 503 9	<LOD 1	<LOD 0.7	125	0.6	9.74	0.2	<LOD 0.3
OCH275- Moana	D	596 9	<LOD 4	386 3	119 2	163 1	2118 4	63 331 11	<LOD 1	61.2 0.9	<LOD 0.5	<LOD 0.2	<LOD 0.2	<LOD 0.3	37.7 0.7
OCH254- Moana	B	<LOD 6	<LOD 2	<LOD 1	<LOD 0.9	<LOD 0.6	81.7 1	6242 4	<LOD 0.9	<LOD 0.7	<LOD 0.4	<LOD 0.5	<LOD 0.3	<LOD 0.6	
OCH020- Moana	D	<LOD 7	<LOD 4	1066 4	<LOD 1	<LOD 0.7	153 2	8949 5	<LOD 1	<LOD 0.7	<LOD 0.5	2.34	0.2	<LOD 0.3	1.6 0.6
OCH036- Moana	C	<LOD 6	<LOD 4	759 3	<LOD 1	<LOD 0.6	<LOD 1	3461 3	<LOD 1	<LOD 0.7	<LOD 0.5	5.6	0.2	3.89	0.3
OCH037- Moana	C	371 8	<LOD 4	394 3	<LOD 1	50.2 0.9	853 3	32 171 8	<LOD 0.9	<LOD 0.7	<LOD 0.4	25.9	0.3	<LOD 0.3	2.9 0.6
OCH036- Moana	B	<LOD 5	<LOD 2	<LOD 0.8	<LOD 0.5	<LOD 0.9	827 2	<LOD 0.9	<LOD 0.7	<LOD 0.4	<LOD 0.4	0.11	0.2	<LOD 0.3	<LOD 0.6



Table 1 (Cont'd.)

ID	Site	Ca	Sc	Ti	V	Cr	Mn	Fe	Cu	Zn	As	Rb	Sr	Pb	LOD								
OCH294	Moana	<LOD 6	<LOD 2	<LOD 1	<LOD 0.8	<LOD 0.6	<LOD 1	2928	3	<LOD 0.9	<LOD 0.7	<LOD 0.4	2.83	0.2	<LOD 0.3	<LOD 0.6							
OCH020-	Moana	<LOD 11	<LOD 5	841	4	<LOD 1	<LOD 0.8	418	2	5849	3	<LOD 1	<LOD 0.9	<LOD 0.6	25.4	0.3	65.7	0.3					
C	OCH101- Moana N-6 (sample 2)	<LOD 12	<LOD 12	302	4	<LOD 2	<LOD 1	2063	4	20 309	9	<LOD 2	<LOD 1	72.6	1	138	0.6	64.9	0.5				
C	OCH050 Pukatoo	931.5	35	4	9	1703	5	1373	3	374	2	22 758	8	251 427	1.3	<LOD 2	60.8	2	36.6	0.4			
OCH024- Pukatoo	A	<LOD 17	<LOD 8	910	6	<LOD 4	9.8	3	6152	10	60 005	14	<LOD 2	<LOD 1	<LOD 1	75.1	0.4	33.1	0.5				
OCH024- Pukatoo	B	618	10	45	5	467	4	646	2	321	2	3690	5	120 830	11	<LOD 1	<LOD 0.8	<LOD 0.6	3.13	0.2			
OCH050- Pukatoo	A	<LOD 7	<LOD 3	<LOD 2	<LOD 1	3.3	0.8	456	2	18 219	6	<LOD 0.9	<LOD 0.7	<LOD 0.5	<LOD 0.2	<LOD 0.3	6	0.6					
OCH067 Wilge Mia	30 552 34	<LOD 9	1011	5	76.4	3	215	2	5909	6	135 746	13	<LOD 2	<LOD 1	<LOD 0.8	<LOD 0.3	<LOD 0.3	45.6	1				
OCH260 Wilge Mia	4157	16	<LOD 4	<LOD 3	<LOD 1	<LOD 1	880	3	23 843	8	<LOD 1	<LOD 0.9	<LOD 0.6	<LOD 0.3	<LOD 0.3	<LOD 0.8							
OCH063 Wilge Mia	52 403 44	<LOD 11	1448	6	202	3	375	2	8838	8	210 901	13	<LOD 2	<LOD 1	<LOD 0.9	<LOD 0.3	<LOD 0.3	107	1				
OCH117- Wilge Mia	A	30 397 33	<LOD 9	1021	5	46.8	3	131	2	12 120	8	183 097	12	<LOD 2	<LOD 1	<LOD 0.9	<LOD 0.3	<LOD 0.3	94.2	1			
OCH118- Wilge Mia	A	38 576 37	<LOD 10	1547	6	234	3	261	2	14 918	9	233 004	12	<LOD 2	<LOD 1	<LOD 1	<LOD 0.3	<LOD 0.4	173	1			
OCH258- Wilge Mia	A	4258	17	<LOD 6	1048	4	<LOD 2	<LOD 1	1919	3	26 701	9	<LOD 1	<LOD 1	<LOD 0.6	<LOD 0.3	<LOD 0.3	<LOD 0.7					
OCH277 Wilge Mia	A	27 329 33	<LOD 8	803	5	97.7	3	213	2	5945	7	129 713	13	<LOD 2	<LOD 1	<LOD 0.8	<LOD 0.3	<LOD 0.3	44.3	1			
OCH257 Wilge Mia	E	20 611 30	<LOD 7	566	4	17	2	139	2	4424	6	97 080	13	<LOD 2	<LOD 1	<LOD 0.7	<LOD 0.3	<LOD 0.3	16.3	1			
OCH061 Wilge Mia	OCH117- Wilge Mia	<LOD 17	<LOD 5	50	3	72.3	2	19.4	1	6935	4	67 894	10	<LOD 1	<LOD 1	<LOD 0.6	19.9	0.3	21.9	0.3			
OCH064- Wilge Mia	A	<LOD 22	263	6	810	3	529	2	213	1	17 044	5	175 920	13	<LOD 1	<LOD 1	<LOD 0.6	25.2	0.3	16.9	0.3		
OCH264- Wilge Mia	A	<LOD 13	<LOD 5	566	3	<LOD 1	<LOD 0.9	2688	2	25 931	6	<LOD 1	<LOD 0.9	<LOD 0.6	<LOD 0.6	22.9	0.3	30.2	0.3	31.6	0.7		
OCH065- Wilge Mia	A	<LOD 12	<LOD 6	453	5	214	2	88	1	9979	3	99 019	9	<LOD 2	<LOD 1	19.7	0.8	25.4	0.4	27	0.5		
OCH117- Wilge Mia	E	<LOD 8	<LOD 4	620	3	1.8	1	64.5	1	947	3	35 025	9	<LOD 1	<LOD 0.8	3	0.5	<LOD 0.2	<LOD 0.3	<LOD 0.6			
OCH117- Wilge Mia	Y	2708	14	675	7	1360	6	983	3	913	2	9350	8	330 997	11	<LOD 1	<LOD 0.7	<LOD 0.8	40	0.3	<LOD 0.2	66.9	1
OCH277- Wilge Mia	A	<LOD 5	<LOD 2	<LOD 1	<LOD 0.8	<LOD 0.6	<LOD 1	2816	3	<LOD 0.9	<LOD 0.7	<LOD 0.7	<LOD 0.4	<LOD 0.4	<LOD 0.2	<LOD 0.3	<LOD 0.6						
OCH065- Wilge Mia	B	243	9	<LOD 4	711	3	<LOD 1	11.8	0.8	404	2	17 692	6	<LOD 1	<LOD 0.7	<LOD 0.4	<LOD 0.2	<LOD 0.3	<LOD 0.6				
OCH260- Wilge Mia	A	174	9	<LOD 4	309	3	218	2	234	1	2516	4	86 304	11	<LOD 1	<LOD 0.7	<LOD 0.5	1.2	0.2	<LOD 0.2	52.7	0.7	
OCH264- Wilge Mia	C	<LOD 7	<LOD 3	293	3	<LOD 1	7.5	0.8	402	2	17 422	6	<LOD 1	<LOD 0.7	<LOD 0.4	1.35	0.2	<LOD 0.3	<LOD 0.6				
OCH119 Wilge Mia	N-2b	3732	21	1330	12	2460	9	1525	5	853	4	34 757	15	449 933	14	<LOD 2	<LOD 1	<LOD 1	60.5	0.5	<LOD 0.4	886	2

demonstrate similar Fe elemental maps to the Nobbs samples. More recent samples OCH283-293 have a similar Fe distribution and profile except OCH 289 however samples 283-293 are similar to OCH-037. Samples OCH 275 and OCH 281 and OCH 254 are also listed as being from Moana, however they are from the Archaeology and Ethnography collections rather than from a specific researcher survey. Care needs to be taken in the interpretations of these samples as they may not be true source samples, rather examples of ochre collected from an archaeological excavation. Therefore these samples are not representative of the site but perhaps artefact ochre found at the site that had been imported from elsewhere. These samples provide examples as potential "unknowns" for attribution to determined source locations established in this study.

### Pine Point

Similarly to Moana, this site is a coastal weathered site and the relatively low Fe concentrations reflect this. As samples OCH299-309 were sampled directly from the site, they represent the variability within the areas sampled. OCH047 and 048 are from the Nobbs collection and bear more similarity to each other than the other samples, reflecting differing sampling campaigns.

### Wilgie Mia

Wilgie Mia and Little Wilgie Mia are both banded iron formations located in Western Australia. A recent paper characterised these materials in the bulk using LA-ICP-MS.<sup>17</sup> The samples from the site again reflect at least three different sampling trips, from Nobbs, Smith and the Western Australian Museum, in order of oldest to most recent. In general the samples are relatively rich in Fe, especially samples such as OCH 117-Y, 260-A and 119, which are composed of high Fe concentration with tightly packed small particles. In contrast OCH 277 and 257, collected by Nobbs, and from the collections of the South Australian Museum, respectively are very low Fe and perhaps not representative of the site.

In general across the five sites discussed, the distribution of the Fe in the samples allows insight into the relationship of the Fe to particular particle sizes and shapes, rather than a bulk analysis. In previous analyses, a distribution in the bulk composition was also observed, with the concentration of Fe ranging from 10–60% iron oxides, depending on the site and mixture.<sup>6,7</sup> The large range of Fe composition in the samples as well as several samples having a very low concentration of Fe calls into question the definition of ochre as far as the majority composition of Fe oxides of the material. As ochre is an admixture of Fe-oxides and other minerals, the varying ratios of these materials and types of materials affect the distribution. Elemental analysis cannot provide direct information on the mineralogical state of the material; therefore some Fe-oxides may be hematite or goethite-based.

### Ca

Ca was an element of interest as at least one site (Bookartoo), the ochre material is found within a dolomite  $[\text{CaMg}(\text{CO}_3)_2]$

matrix.<sup>27</sup> Semiquantitative values of Ca ranged from below detection limits up to 9%. Previous archaeometric studies had identified Ca as a discriminatory element for this site.

From previous analyses, Bookartoo is known for its relatively high Fe, Ca and V concentrations.<sup>27</sup> The microelemental analysis supports these conclusions from the bulk chemical analyses, however the concentration and distribution across the samples is not consistent. Karrku, Moana and Pine Point have very little Ca, however Wilgie Mia has Ca associated with both small rounded and large angular particles. There is a direct correlation between the Fe and Ca in both Bookartoo and Wilgie Mia samples suggesting that during deep weathering of the sites the Fe oxides may have reacted with the dolomite or calcite to form ankerite  $\text{CaFe}(\text{CO}_3)_2$ , the Fe analogue of dolomite.<sup>16,31,32</sup>

While not exhaustive of every site in Australia these results suggest that Ca is indicative with banded iron formations within covered deposits or related formations, and not as associated with weathered, exposed sites. For this sample set, Ca is one of a few clear discriminatory elements for Bookartoo and Wilgie Mia and is characteristic of these sites in higher concentrations.

### Rb

Rb was an element that ranged from below detection limits to 212 ppm in the sites examined, and was detected in most of the samples analysed (Table 1).

However, essentially very little Rb was identified in the Bookartoo or Wilgie Mia ochre samples, and therefore it is not associated with Fe or other Fe-bearing minerals from the site.

Moana has variability with the samples in the concentration of Rb. The higher concentrations of Rb appear to be associated with larger, angular particles rather than smaller rounded particles. Similarly to Moana, Karrku also has Rb associated with the larger angular particles, but this is not universally found across all samples from the site.

Pine Point ochre samples have some distribution of Rb, particularly in the larger particles in samples OCH302, 303 and 304, which represent a particular sampling location within the site. OCH 309 and 310, 299 and 048 do not have the same distribution of Rb, reflecting the diversity of the ochre material within the site.

### Other elements

Images of elemental maps of the slides with elements that were less consistently observed will not be discussed as extensively as the above elements. These include As, Ti and Mn.

For As, most samples are devoid of even low concentrations of As, with the exception of OCH254-A, OCH101-C and OCH275-C from Moana. As discussed earlier, these samples may be related to the archaeology of the site rather than being examples of source samples.

Ti is not in high concentration or distribution for the sites with the exception of Wilgie Mia. The amount of Ti in the sample is not necessarily related to the sampling campaign for these. Of these samples, OCH062, 062-A and 063, 067, 065 (Western Australia Museum) and 119, 117-Y, 117-A and 119



(Mike Smith) have relatively high concentrations of Ti. However, OCH 260 (Mike Smith) and 065-A (WA Museum) do not. As discussed earlier, this reflects the large scale of the site and the possibilities of the sampling locations. Titanium can occur at low levels in hematite, but can also be present as one of the  $TiO_2$  polymorphs of are ilmenite ( $FeTiO_3$ ), which are widespread detrital minerals in sediments.

Both Cr and Mn have similar distributions patterns to Fe in the ochre samples, with similar trends in concentration and distribution. This indicates they are present substituting into hematite and magnetite. The distributions of these elements will not be discussed in depth.

### Tri-elemental images

One of the strengths of the XFM technique combined with GeoPIXE is the ability to generate elemental maps of three elements simultaneously. This “overlaid” of elemental maps allows clear differentiation of correlation and anti-correlation of elements as well as the relationship of elemental concentration to a particle or particles or features in the sample. As with the

single element plots, the individual elements are falsely coloured to indicate concentration intensity. Using the three colours of red, green and blue, the elements can be easily identified as well as mixtures (e.g. equal amounts of red and blue generate purple regions). As there were many combinations of elements, the combination of Ca (red), Fe, (green) and V (blue) was a representative example.

Visualising the samples in this context allows more interpretation of the elemental distribution for each sample type. In this combination, Karrku, Moana, Pine Point and Wilgie Mia generally are composed of varying concentrations of Fe. However, Bookartoo is revealed to be a complex mixture of Ca, Fe and V, especially in cases such as OCH 255-2 and 255-4 where elemental concentrations can be attributed to individual particles. Moana samples OCH 254, 281 and 275 as attribution case study examples provide a revealing story. The tri-elemental plots allow for characterisation using three discriminatory elements. Moana does not necessarily have a clear elemental profile or definition; rather three to four patterns are seen in the particle size and elemental concentrations. As seen at the site itself, Moana is a large distribution of red and yellow formations with



Fig. 7 Microelemental map of Ca, Fe and V for all 165 samples analysed in this study. Red indicates Ca, green indicates Fe and blue indicates V. Images are false coloured to demonstrate relative concentration intensities, with black the lowest and the indicated colour the highest.

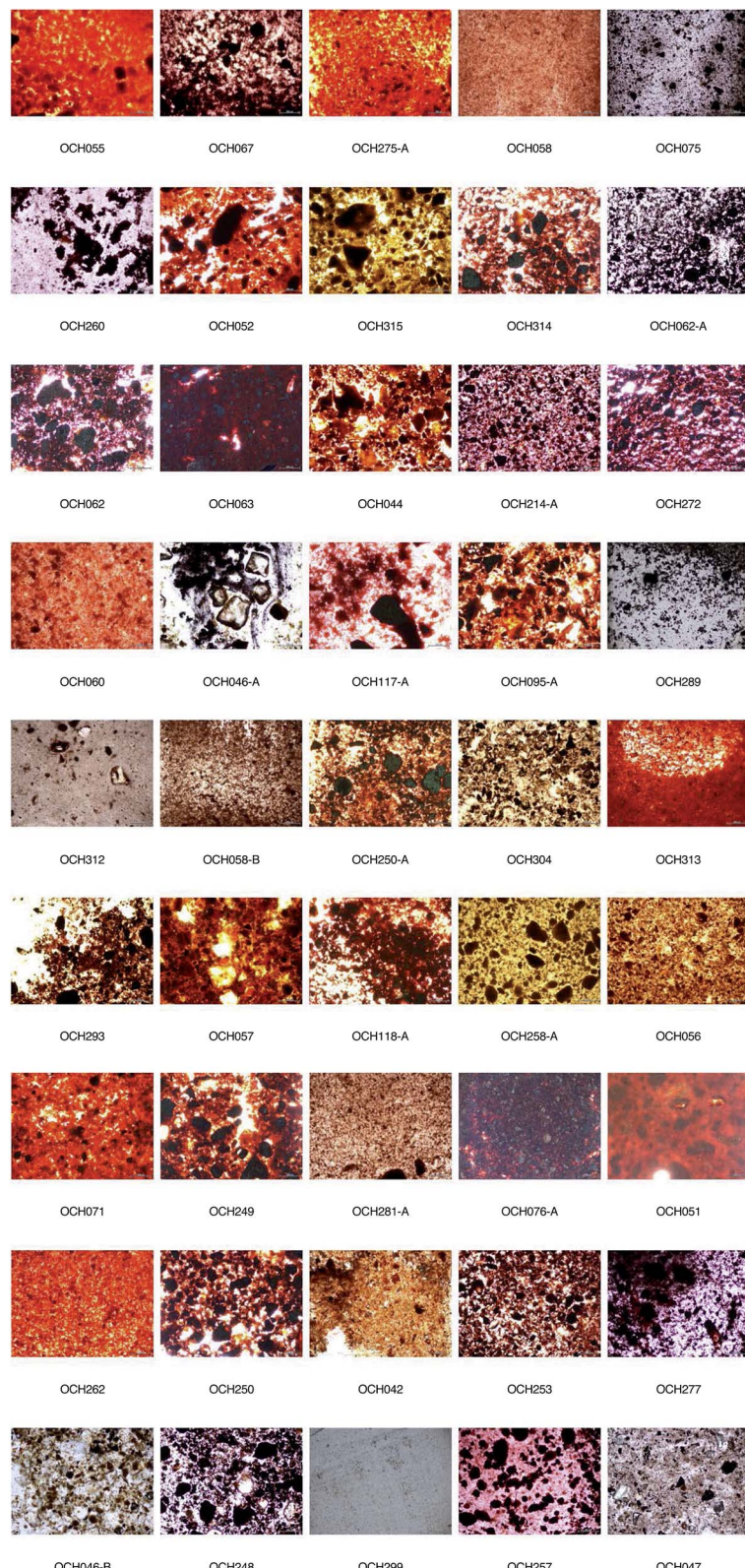


Fig. 8 (contd.)



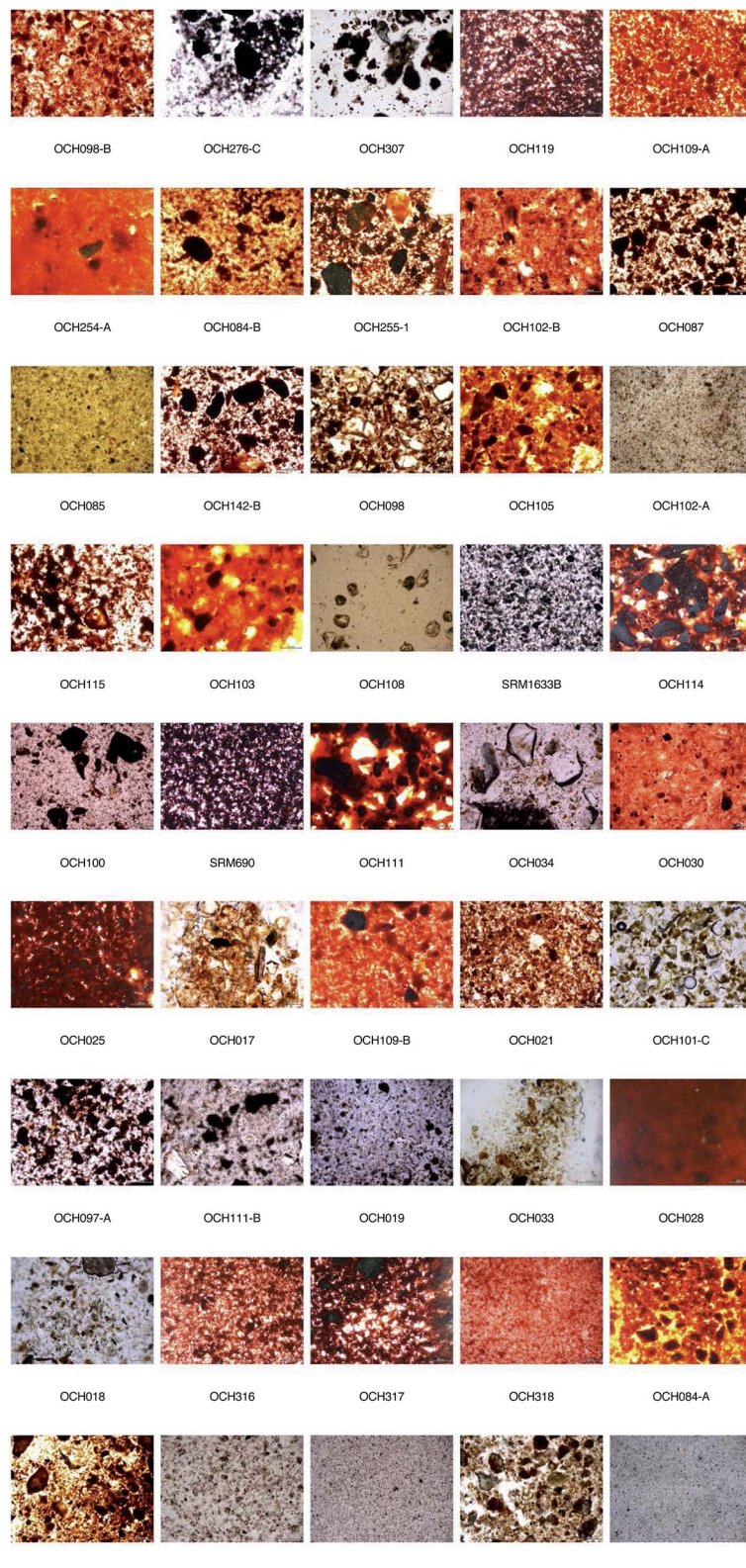


Fig. 8 (contd.)



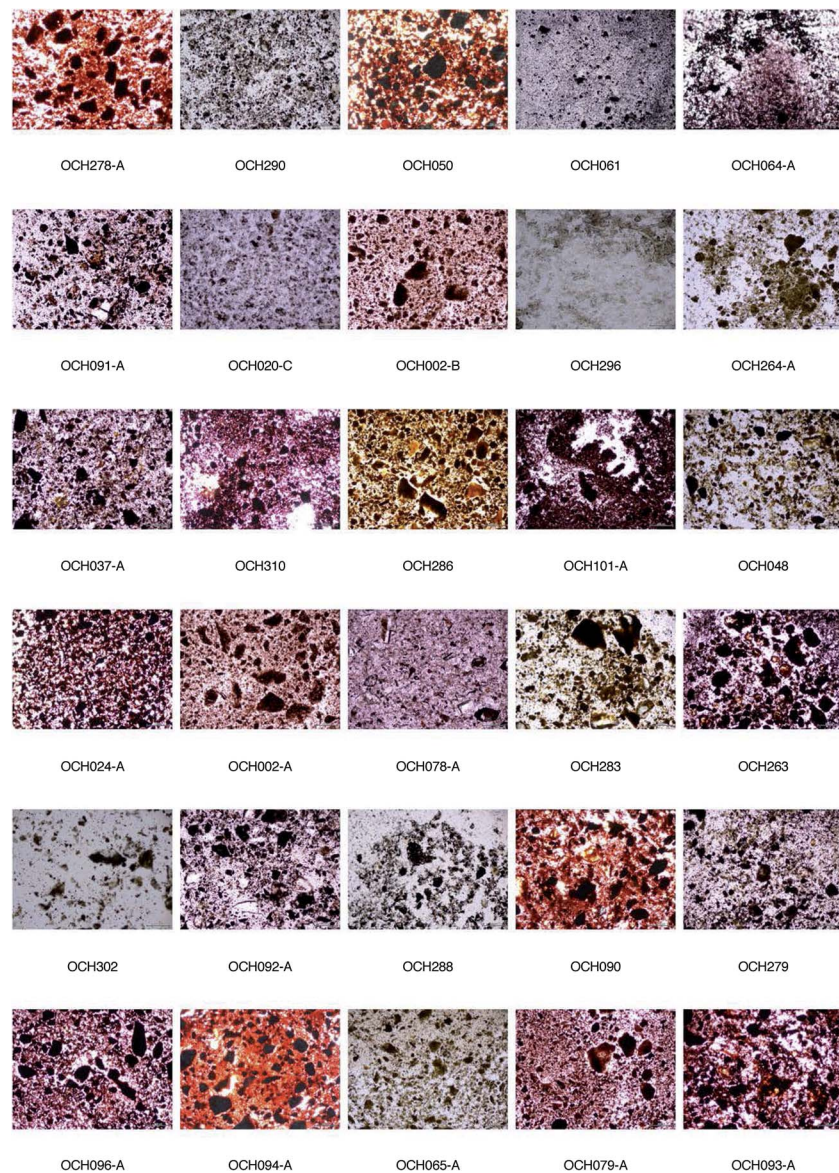


Fig. 8 (contd.)



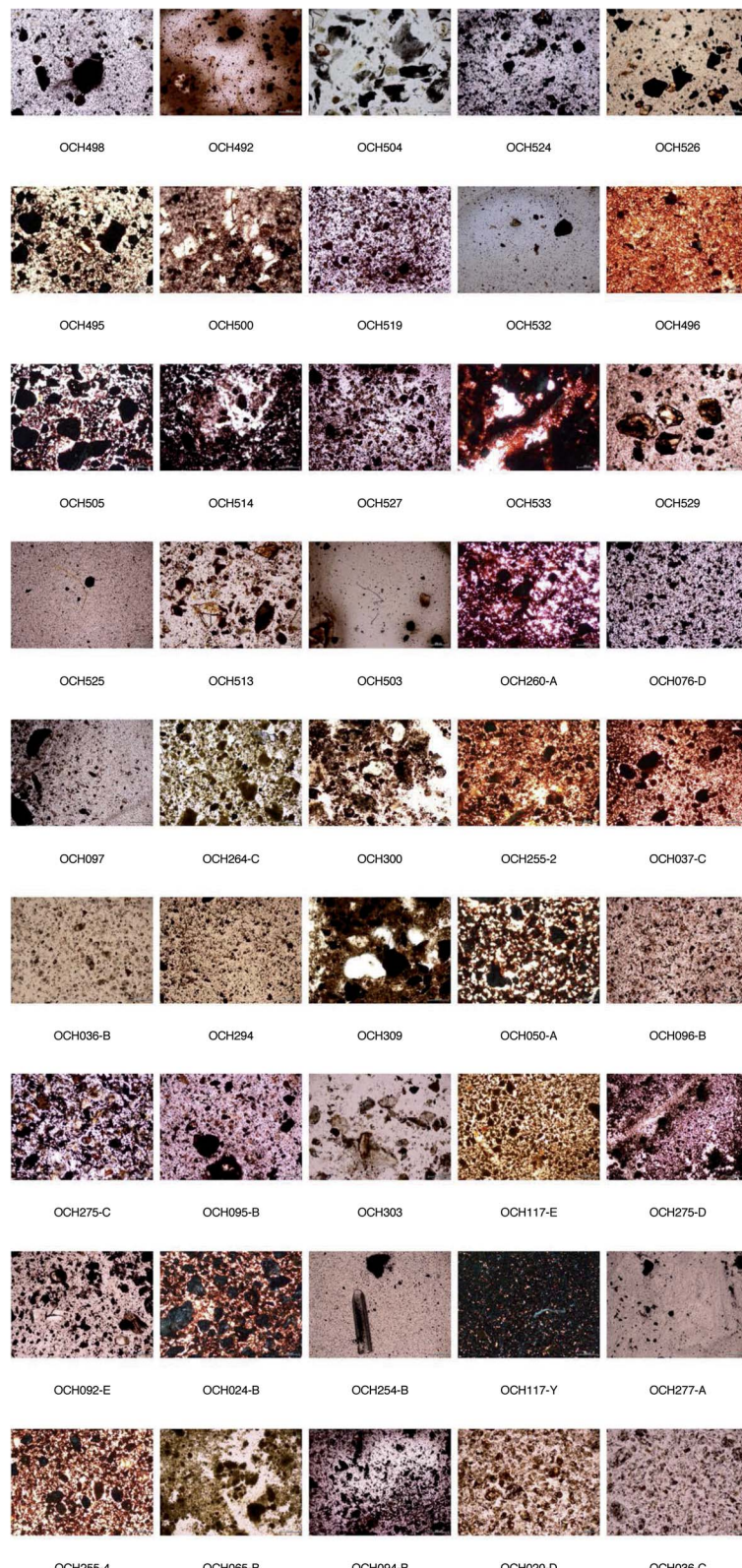


Fig. 8 Transmitted light microscopy of the same slides analysed by XFM at 100 $\times$  magnification. The scale bar is 200 micron for each image. Images are arranged in the same order, as on the slide. (a) Slide A1 (b) Slide A2 (c) Slide A3 (d) Slide B1.

differing characteristics. Unlike Bookartoo, the diversity of the Moana site makes it more difficult to attribute an archaeological “unknown” to the site, whereas this attribution would be easier with a sample from Bookartoo or Wilgie Mia.

Fig. 7 displays the tri-elemental plot of Ca, Fe and V for all 165 elements analysed. These data represent a large variety of deposits and sites from across Australia. This figure demonstrates the great diversity of deposit chemistry and particle distribution and sizes.

### Light microscopy

With visual inspection of the slides it can be observed that for several samples there is a very low amount of ochre sample within the epoxy resin (Fig. 8). Therefore the elemental maps with low concentrations of Fe are more representative of the relatively few particles of ochre rather than a low concentration of a particular element in the particles. This relatively low concentration may be a reflection of the properties of mixing of the material with the resin; therefore mixing of the same material with another traditional paint binder such as water, natural resin, or proteinaceous binder may have a different effect on the number of particles in suspension.<sup>4</sup> In addition, as all samples were pre-sieved to less than 250 micron, it may be the case that the ochre samples from these sites have more particles larger than 250 micron.

The colour of the individual ochre sample can also be observed for each sample. Most examples are in the traditional palette of reds, oranges, yellows and browns and even some purple samples. The colour and particle shape variability can also be observed within the individual samples and between samples from the same site. For instance, OCH024 and 255-A (B1) demonstrate the deep red colour and mixture of intense fine particles (5–10 micron) along with the larger “platy” dark particles (200 micron) characteristic of the site. However, OCH 101-C (A2, Moana) contains a collection of yellow spherical particles on the order of 50–100 micron. The particle colour as well as the shape influence the overall colour when viewed by eye, and the elemental composition in combination with lighter elements such as Ca, O, Si, K and others form the original mineralogy of the material. Viewing this microscopic palette of the 165 samples analysed in this study gives a comprehensive view into the diversity of minerals and mineral mixtures that compose Australian ochre.

## Conclusions

This study demonstrates the first successful use of X-ray fluorescence microanalysis towards the characterisation of multiple Australian Aboriginal ochre samples from across Australia. Samples from cultural areas including both sources and archaeological contexts provide a wide-ranging data set to examine the variability within and between site locations. The micron-scale elemental maps produced in this work provide compositional and spatial information on the distribution of minerals in complex pigment materials that are not available in bulk techniques. The results from this study support earlier

bulk technique data on the elemental characterisation of ochre samples, and supports the need for sensitive multielemental techniques to fully understand this complex and variable material. Semiquantitative data from GeoPIXE also aids in understanding elemental trends in the samples for a standardised area on a sample slide.

As each sample is representative of a small area of an ochre source with inherent variability due to genesis and site history, one sample from each site cannot be considered representative of a large site location. As demonstrated in this study, some sites such as Bookartoo the deposits are relatively consistent, whereas for a site such as Moana where diagenetic processes have altered the site has a more diverse elemental and mineral profile. Rather, the combination of source samples using multiple elements allows characterisation down to the association of elemental profile with single particles. In addition, the presence or absence of a single element is not indicative of a particular source location; rather a combination of elements and concentrations as well as elements relative to a particular particle pattern aid in the characterisation of the material from a particular site. The addition of light microscopy of the same areas elementally analysed provides a fuller picture of the particle colours and distribution. This study assists in the attribution of ochre to original sites, aiding in the understanding of the cultural uses and potential exchange of ochre, however assignments of samples to particular cultural locations must be made with care and with an understanding of both the chemistry and cultural context. Future studies include expansion of the database of deposits and archaeological sites and application to artefacts.

## Acknowledgements

We gratefully acknowledge the South Australian Museum Board and South Australian Museum Aboriginal Advisory Group for support and permission to access and analyse the collections. We also thank the staff at the South Australian Museum Aboriginal Australian Collections for access to the collections. We are also grateful to Mike Smith and other collaborators for access to their collections for analysis. We acknowledge the preparation of the epoxy cast samples by Ms Caroline Watson and Mr Owen Osborne. The staff at Pontifex, Kensington, South Australia are gratefully acknowledged for their careful final preparation of the slides. We acknowledge Professor Paul Kirkbride, Flinders University for the use of the microscope. The project has approval number 4670 from the Social and Behavioural Research Ethics Committee of Flinders University. Funding is gratefully acknowledged from Australian Institute of Nuclear Science and Engineering (AINSE) Research Fellowship (Popelka-Filcoff), and Australian Research Council Grant #LP0882597 (Lenehan, Pring and Popelka-Filcoff). Part of this research was undertaken on the XFM beam line at the Australian Synchrotron, Victoria, Australia.

## Notes and references

- 1 P. Nel, P. A. Lynch, J. S. Laird, H. M. Casey, L. J. Goodall, C. G. Ryan and R. J. Sloggett, *Nucl. Instrum. Methods Phys. Res., Sect. A*, 2010, **619**, 306–310.



2 P. S. C. Tacon, in *Soils, Stones and Symbols: Cultural Perceptions of the Mineral World*, ed. N. O. M. A. Boivin, UCL Press, London, 2004, pp. 31–42.

3 A. J. Blee, K. Walshe, A. Pring, J. S. Quinton and C. E. Lenehan, *Talanta*, 2010, **82**, 745–750.

4 T. Reeves, R. S. Popelka-Filcoff and C. E. Lenehan, *Anal. Chim. Acta*, 2013, **803**, 194–203.

5 R. M. Cornell and U. Schewertmann, *The Iron Oxides*, Wiley-VCH Verlag GmbH &Co., Weinheim, 2003.

6 R. S. Popelka-Filcoff, C. Lenehan, K. Walshe, J. W. Bennett, A. Stopic, P. Jones, A. Pring, J. S. Quinton and A. Durham, *Journal of the Anthropological Society of South Australia*, 2012, **35**, 81–90.

7 R. S. Popelka-Filcoff, C. E. Lenehan, M. D. Glascock, J. W. Bennett, A. Stopic, J. S. Quinton, A. Pring and K. Walshe, *J. Radioanal. Nucl. Chem.*, 2012, **291**, 19–24.

8 R. S. Popelka-Filcoff, A. Mauger, C. E. Lenehan, K. Walshe and A. Pring, *Anal. Methods*, 2014, **6**, 1309–1316.

9 U. Bergmann, P. L. Manning and R. A. Wogelius, in *Annual Review of Analytical Chemistry*, ed. R. G. Cooks and E. S. Yeung, Annual Reviews, Palo Alto, 2012, vol. 5, pp. 361–389.

10 L. Bertrand, L. Robinet, M. Thoury, K. Janssens, S. Cohen and S. Schöder, *Appl. Phys. A*, 2012, **106**, 377–396.

11 D. L. Howard, M. D. de Jonge, D. Lau, D. Hay, M. Varcoe-Cocks, C. G. Ryan, R. Kirkham, G. Moorhead, D. Paterson and D. Thurrowgood, *Anal. Chem.*, 2012, **84**, 3278–3286.

12 K. Janssens, J. Dik, M. Cotte and J. Susini, *Acc. Chem. Res.*, 2010, **43**, 814–825.

13 L. Monico, G. van der Snickt, K. Janssens, W. de Nolf, C. Miliani, J. Dik, M. Radepont, E. Hendriks, M. Geldof and M. Cotte, *Anal. Chem.*, 2011, **83**, 1224–1231.

14 R. L. Green and R. J. Watling, *J. Forensic Sci.*, 2007, **52**, 851–859.

15 M. Jercher, A. Pring, P. G. Jones and M. D. Raven, *Archaeometry*, 1998, **40**, 383–401.

16 M. Smith and B. Fankhauser, *Geochemistry and identification of Australian red ochre deposits* National Museum of Australia and Centre for Archaeological Research, Canberra, 2009.

17 R. Scadding, V. Winton and V. Brown, *J. Archaeol. Sci.*, 2015, **54**, 300–312.

18 D. C. Creagh, M. E. Kubik and M. Sterns, *Nucl. Instrum. Methods Phys. Res., Sect. A*, 2007, **580**, 721–724.

19 P. Jones, *Journal of the Anthropological Society of South Australia*, 1984, **22**, 3–10.

20 P. Jones, *Journal of the Anthropological Society of South Australia*, 1984, **22**, 10–19.

21 P. Jones, *Ochre and Rust: Artefacts and Encounters on Australian Frontiers*, Wakefield Press Adelaide, 2007.

22 P. Jones and P. Sutton, *Art and Land: Aboriginal Sculptures of The Lake Eyre Region*, South Australian Museum and Wakefield Press, Adelaide, Australia, 1986.

23 M. F. Nobbs, Aboriginal painters of the Olary District of South Australia an ethnoecological study of the Lake Frome Plains and the adjoining uplands, with particular reference to the granite area of the Olary Uplands/By Margaret Nobbs, History, 1995, 1996.

24 R. Popelka-Filcoff, C. Lenehan, M. Glascock, J. Bennett, A. Stopic, J. Quinton, A. Pring and K. Walshe, *J. Radioanal. Nucl. Chem.*, 2012, **291**, 19–24.

25 M. A. Smith and B. Fankhauser, *An archaeological perspective on the geochemistry of Australian red ochre deposits: Prospects for fingerprinting major sources*, Australian Institute of Aboriginal and Torres Strait Islander Studies, Canberra, 1996.

26 M. A. Smith and S. Pell, *J. Archaeol. Sci.*, 1997, **24**, 773–778.

27 J. L. Keeling, *Geological Survey: Bookartoo Ochre Deposit Sec. 85 HD. Parachilna 831*, Department of Mines and Energy, South Australia, 1984.

28 N. Paterson and R. Lampert, *Rec. Aust. Mus.*, 1985, **37**, 1–9.

29 J. Clarke, *Stud. Conserv.*, 1976, **21**, 134–142.

30 C. G. Ryan, R. Kirkham, R. M. Hough, G. Moorhead, D. P. Siddons, M. D. de Jonge, D. J. Paterson, G. de Geronimo, D. L. Howard and J. S. Cleverley, *Nucl. Instrum. Methods Phys. Res., Sect. A*, 2009, **619**, 37–43.

31 J. Clarke and N. North, in *Rock Art and Posterity: Conserving, Managing and Recording Rock Art*, ed. C. Pearson and B. K. Swartz Jr., Australian Rock Art Research Association, Melbourne, 1991, pp. 80–87.

32 J. Clarke and N. North, in *Rock Art and Posterity: Conserving, Managing and Recording Rock Art*, ed. C. Pearson and B. K. Swartz Jr., Australian Rock Art Research Association, Melbourne, 1991, pp. 88–92.

